Journal of Power Sources 245 (2014) 482–486

Contents lists available at SciVerse ScienceDirect

Journal of Power Sources

journal homepage: www.elsevier.com/locate/jpowsour

Short communication

Enhancement of electrocatalytic performance of hydrogen storage alloys by multi-walled carbon nanotubes for sodium borohydride oxidation

Dongming Zhang, Guiling Wang, Kui Cheng, Jichun Huang, Peng Yan, Dianxue Cao*

Key Laboratory of Superlight Material and Surface Technology of Ministry of Education, College of Material Science and Chemical Engineering, Harbin Engineering University, Harbin 150001, PR China

HIGHLIGHTS

- High electrocatalytic performance, 500 mA cm^{-2} at −0.3 V in 0.5 mol dm^{-3} $NaBH_4$.
- Hydrogen adsorption capacity of AB_5 was improved by the addition of MWNTs.
- Investigation for the role of MWNTs in $NaBH_4$ electrooxidation.

ARTICLE INFO

Article history:
Received 5 May 2013
Received in revised form
27 June 2013
Accepted 28 June 2013
Available online 6 July 2013

Keywords:
Hydrogen storage alloy
Multi-walled carbon nanotubes
Borohydride electrooxidation
Direct borohydride fuel cell

ABSTRACT

Catalytic electrodes consisting of $MmNi_{0.58}Co_{0.07}Mn_{0.04}Al_{0.02}$ (AB_5-type alloy) and multi-walled carbon nanotubes (MWNTs) are studied for $NaBH_4$ electrooxidation and are characterized by scanning electron microscope and X-ray diffractometer. The $NaBH_4$ electrooxidation performance on the AB_5/MWNTs electrode is tested by cyclic voltammetry and chronoamperometry methods. The electrode performance is significantly affected by the content of MWNTs and the optimized content of MWNTs is found to be 2 wt.%. The steady state current density for $NaBH_4$ electrooxidation at the AB_5/MWNTs (2 wt.%) electrode is about twice of that at the AB_5 electrode without MWNTs. The utilization efficiency of $NaBH_4$ at the AB_5/MWNTs electrode is 61.5% higher than that at the pristine AB_5 electrode. The enhanced electrocatalytic activity and $NaBH_4$ utilization at the AB_5/MWNTs (2 wt.%) electrode can be attributed to MWNTs, which acts as a hydrogen adsorbent to diminish hydrogen release.

1. Introduction

Direct borohydride fuel cells (DBFCs) have attracted much attention due to their high power density, high open circuit voltage, and low pollution [1–10]. As the fuel of DBFCs, $NaBH_4$ exhibits many advantages, such as, non-flammable, non-CO_2 emission, high hydrogen contents (10.6 wt.%), and high specific capacity (5668 Ah kg^{-1}). The complete electrooxidation of $NaBH_4$ generates 8 electrons (Eq. (1)). However, the hydrolysis (Eq. (2)) and the incomplete electrooxidation of $NaBH_4$ in alkaline solution lead to significant reduction in the utilization of $NaBH_4$ [1–12]. Therefore, it is necessary to develop electrocatalysts that can enhance the utilization of $NaBH_4$ by diminishing the hydrolysis and promoting the complete electrooxidation.

$$BH_4^- + 8OH^- \rightarrow BO_2^- + 6H_2O + 8e^- \quad (1)$$

$$BH_4^- + 2H_2O \rightarrow BO_2^- + 4H_2 \quad (2)$$

Electrocatalysts for borohydride oxidation usually includes precious metals and hydrogen storage alloys [12–29]. The precious metals have high catalytic activity, but they strongly catalyze the hydrolysis of borohydride (Eq. (2)) leading to the reduction of borohydride utilization and the decrease of the energy density of DBFCs [12–21]. Hydrogen storage alloys, on the other hand, have low catalytic activity for the borohydride hydrolysis and they also have the ability to absorb hydrogen formed by electrooxidation or hydrolysis of borohydride (Eqs. (3), (4)), so borohydride electrooxidation on hydrogen storage alloys usually has higher utilization than on precious metal catalysts. Besides, hydrogen storage alloys are cheaper than precious metals. However, the electrocatalytic activity of hydrogen storage alloys is much lower than precious metals.

* Corresponding author. Tel./fax: +86 451 82589036.
E-mail address: caodianxue@hrbeu.edu.cn (D. Cao).

0378-7753/$ – see front matter © 2013 Elsevier B.V. All rights reserved.
http://dx.doi.org/10.1016/j.jpowsour.2013.06.161

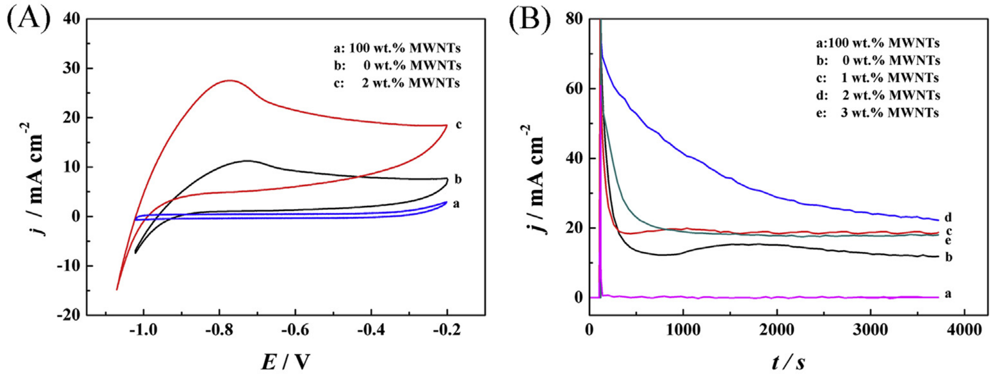

Fig. 1. Cyclic voltammograms of the MWNTs, AB_5 and AB_5/MWNTs (2 wt.%) electrodes in 0.1 mol dm^{-3} $NaBH_4$ + 2.0 mol dm^{-3} NaOH at a scan rate of 5 mV s^{-1} (A) and chronoamperometric curves of the AB_5/MWNTs (*x* wt.%) in 0.1 mol dm^{-3} $NaBH_4$+ 2.0 mol dm^{-3} NaOH at −0.7 V (B).

$$BH_4^- + 2H_2O + M \rightarrow MH_{X,ads} + BO_2^- + (4 - 0.5X)H_2 \quad (3)$$

$$MH_{X,ads} + XOH^- \rightarrow M + XH_2O + Xe^- \quad (4)$$

In order to improve the catalytic performance of hydrogen storage alloys, surface modifications of hydrogen storage alloys have been studied. Wang et al. [24–26] investigated the modification of AB_5-type hydrogen storage alloys with Ti/Zr, Si and Au by ball-milling method. They found that hydrogen evolution was restrained on the hydrogen storage alloys with surface attached Ti/Zr or Si. However, the existence of Ti/Zr, Si and La_2O_3 decreased the catalytic activity for BH_4^- electrooxidation. Wang et al. [26] also found that doping the AB_5-type alloy with Au via a self-reduction method increased the BH_4^- electrooxidation current density from 100 to 175 mA cm^{-2} in 1.0 mol dm^{-3} KBH_4. Our group [28,29] demonstrated that the surface modifications of AB_5-type alloy by Fe_2O_3 and Pd result in enhancements in their catalytic activity for BH_4^- electrooxidation.

Carbon nanotubes have been reported to be able to store hydrogen electrochemically and the stored hydrogen can be electrooxidized [30–32]. In this study, hydrogen storage alloy was combined with MWNTs to form a composite electrode. By taking the advantages of the electrochemical hydrogen storage ability and good electrical conductivity of MWNTs, the composite electrode achieved high catalytic activity for $NaBH_4$ electrooxidation and high $NaBH_4$ utilization. We provided evidences to illustrate that MWNTs plays a significant role in storing hydrogen and increasing hydrogen absorption in AB_5.

2. Experimental

The as-prepared $MmNi_{0.58}Co_{0.07}Mn_{0.04}Al_{0.02}$ (AB_5-type alloy) was provided by Dandong Hongyuan alloy Co. Ltd. China, where Mm is the Mischmetal (an alloy of rare earth elements) consisting of Ce, La, Nd, Pr and trace amount of other elements. The MWNTs (10–20 nm in outer diameter and 5–15 μm in length) were purchased from Shenzhen Nanotech Port Co. Ltd.

The as-prepared AB_5-type alloy powder (400 mesh) was mixed with MWNTs at the mass ratio (Alloy:MWNTs) of 100:0, 99:1, 98:2, 97:3, respectively, in a solution containing 6 wt.% polytetrafluoroethylene (PTFE) and 1.5 wt.% sodium carboxymethyl cellulose (CMC). The mixture was smeared onto a Ni-foam sheet ($10 \times 10 \times 1$ mm) with a point-welded nickel wire as the current collector by a doctor-blade. After drying at 343.15 K for 2.5 h in a vacuum oven, the electrode was pressed under a pressure of 10 MPa. The thickness of the AB_5/MWNTs electrode is about 0.5 mm and the mass of the active material in an electrode is 0.2 g. All electrochemical experiments were carried out in a conventional three-electrode electrochemical cell with a carbon rod (3 mm in diameter) counter electrode and a saturated Ag/AgCl, KCl reference electrode. The system was controlled by a computerized potentiostat (Autolab PGSTAT302, Eco Chemie). All electrochemical measurements were conducted at room temperature under the protection of ultrapure N_2. All solutions were made with analytical grade chemical reagents and ultrapure water (Milli-Q, 18 MΩ cm).

The morphology of the electrodes was determined using a scanning electron microscope (SEM, JEOL JSM-6480). The structure was analyzed by a powder X-ray diffractometer (XRD, Rigaku TTR-III) equipped with Cu Kα radiation ($\lambda = 0.15406$ nm).

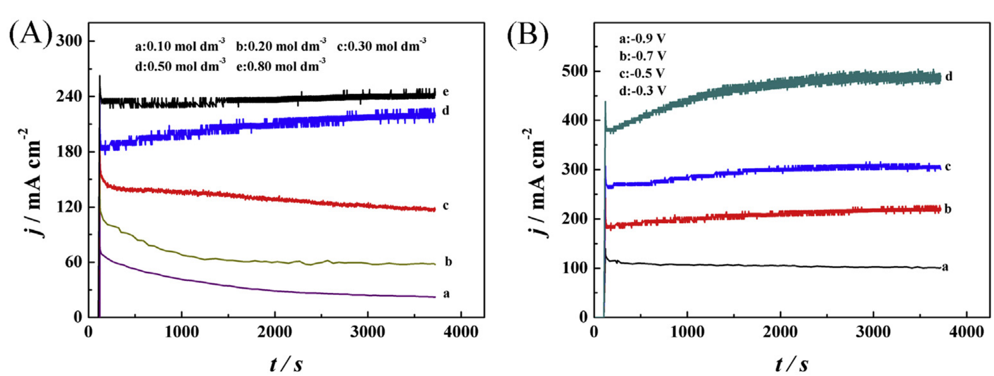

Fig. 2. Chronoamperometric curves of $NaBH_4$ electrooxidation at the AB_5/MWNTs (2 wt.%) electrode in 2.0 mol dm^{-3} NaOH + *x* mol dm^{-3} $NaBH_4$ at −0.7 V (A). Chronoamperometric curves of $NaBH_4$ electrooxidation at the AB_5/MWNTs (2 wt.%) electrode in 2.0 mol dm^{-3} NaOH + 0.5 mol dm^{-3} $NaBH_4$ at different potentials (B).

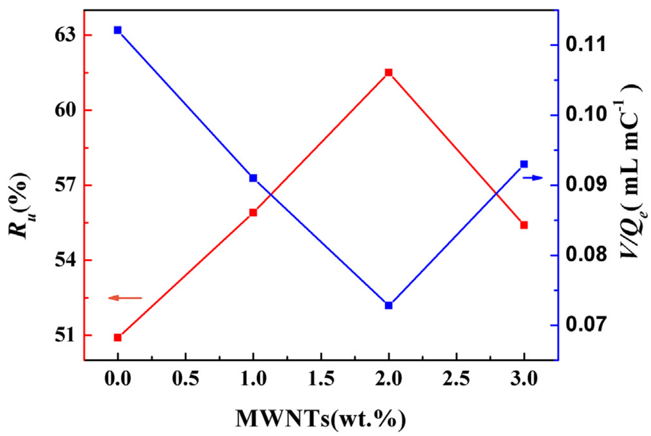

Fig. 3. The $NaBH_4$ utilization and the hydrogen evolution rate at the AB_5/MWNTs (*x* wt.%) electrodes.

3. Results and discussion

3.1. $NaBH_4$ electrooxidation at the AB_5/MWNTs electrode

In order to investigate effects of MWNTs on the catalytic performance of AB_5 alloy for $NaBH_4$ electrooxidation, cyclic voltammograms (CV) of the AB_5/MWNTs composite electrode with 2 wt.% MWNTs, the electrode of AB_5 and the electrode of MWNTs were measured in 2 mol dm^{-3} NaOH and 0.1 mol dm^{-3} $NaBH_4$. The results are shown in Fig. 1(A). As seen, the MWNTs electrode shows nearly no catalytic activity for $NaBH_4$ electrooxidation. The AB_5/MWNTs (2 wt.%) electrode displays a more negative onset potential (−1.02 V) than the AB_5 electrode (−0.96 V). The peak current density of AB_5/MWNTs (2 wt.%) electrode reaches 27 mA cm^{-2}, which is almost 2.5 times that of the AB_5 electrode. Fig. 1(B) shows the chronoamperometric curves (CA) of the AB_5/MWNTs electrode with different MWNTs contents in 0.1 mol dm^{-3} $NaBH_4$ and 2.0 mol dm^{-3} NaOH at a constant potential of −0.7 V. The current density stabilized at around 0 mA cm^{-2} and 12 mA cm^{-2} for the MWNTs and AB_5 electrode, respectively, after reaction for 50 min. The current density is 18, 23 and 17 mA cm^{-2} for the AB_5/MWNTs electrodes with 1, 2 and 3 wt.% MWNTs, respectively, after 50 min reaction. Clearly, the AB_5/MWNTs electrodes exhibited significantly higher catalytic activity than the AB_5 electrode without MWNTs, demonstrating that MWNTs improved the catalytic performance of the AB_5 alloy. The AB_5/MWNTs electrode with 2 wt.% MWNTs shows the best performance among the three samples.

The catalytic activity of the AB_5/MWNTs (2 wt.%) electrode was further investigated by varying the $NaBH_4$ concentration and the oxidation potential. Fig. 2(A) shows the effects of $NaBH_4$ concentration on the catalytic activity. Obviously, with the increase of $NaBH_4$ concentration from 0.1 to 0.8 mol dm^{-3}, the oxidation current density was increased remarkably. After 4000 s reaction in 0.5 mol dm^{-3} $NaBH_4$ at −0.7 V, the current density is 220 mA cm^{-2}, which is more than twice of that at the AB_5 electrode reported in our previous work (95 mA cm^{-2}) [27]. This further indicated that MWNTs enhanced the catalytic activity of the AB_5 alloy. The current density decreased with the reaction time when the $NaBH_4$ concentration is lower than 0.3 mol dm^{-3}, which is likely caused by the concentration polarization. When the $NaBH_4$ concentration is higher than 0.5 mol dm^{-3}, the oxidation current density became quite stable but less smooth, which might result from the release of hydrogen gas. Fig. 2(B) shows the influence of the oxidation potential on the electrocatalytic activity. As seen, the current density after 4000 s reaction in 0.5 mol dm^{-3} $NaBH_4$ increased from 100 to 500 mA cm^{-2} when the potential was increased from −0.9 to −0.3 V. The current–time curve became noisier at higher potential, likely due to the faster hydrogen gas formation rate at higher potentials.

$NaBH_4$ electrooxidation is usually accompanied by the hydrolysis reaction (Eq. (2)) leading to hydrogen evolution and reduction of utilization of $NaBH_4$. In order to examine the effect of MWNTs on the utilization efficiency of $NaBH_4$, we measured the hydrogen

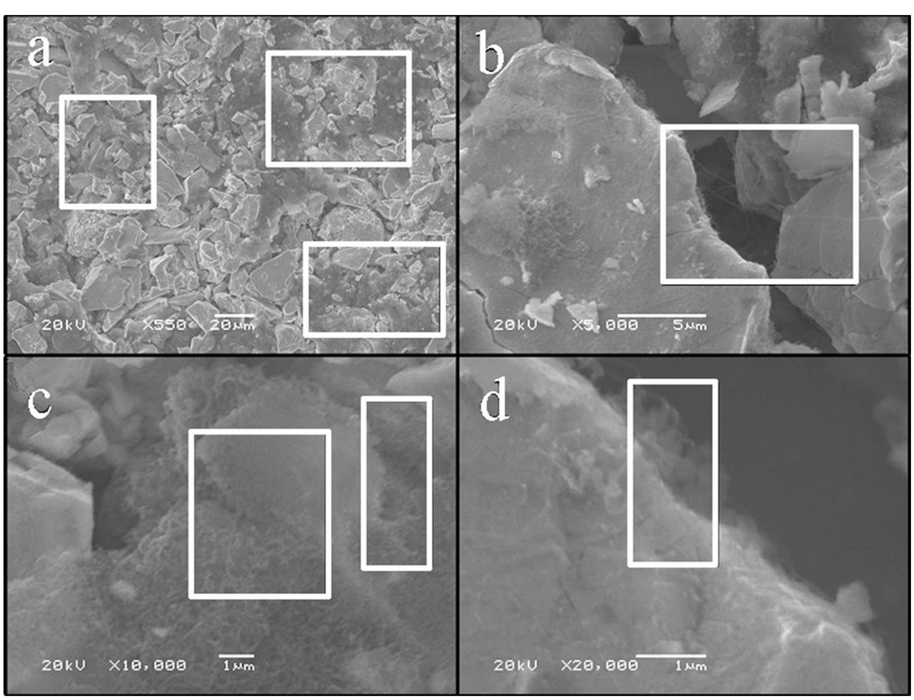

Fig. 4. SEM images of the AB_5/MWNTs (2 wt.%) electrode at different magnification. It has been reported that the absorption of hydrogen in AB_5 alloy results in crystal.

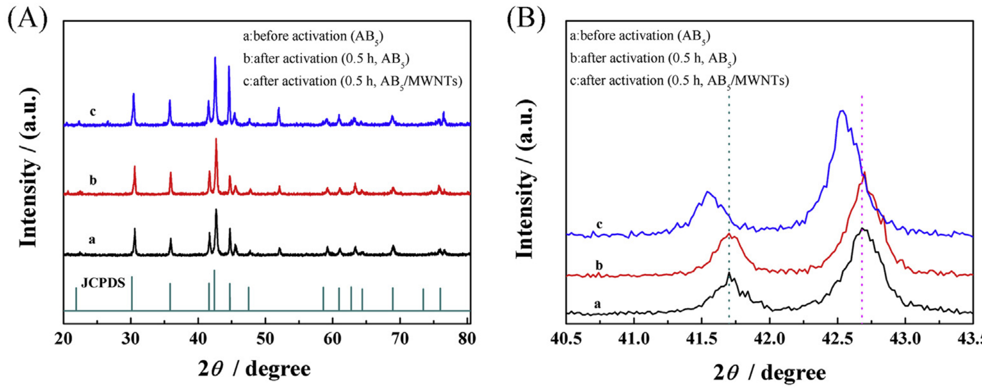

Fig. 5. XRD patterns of the pristine AB_5 alloy, the AB_5 and the AB_5/MWNTs treated in 0.1 mol dm^{-3} $NaBH_4$ + 6 mol dm^{-3} NaOH for 0.5 h (A) and the enlargement in the 2θ range of 40.5°–43.5° (B).

evolution rate and calculated the $NaBH_4$ utilization at the AB_5/MWNTs and the AB_5 electrode using Eq. (5) [24]:

$$R_u\% = \frac{Q_e}{Q_e + Q_h} \times 100\% \tag{5}$$

where, Q_e represents the electrical charge obtained from the integration of the chronoamperometric curves in Fig. 1(B). Q_h is the charge calculated from the volume of hydrogen collected by a conventional water replacement method during the reaction. Fig. 3 shows effects of MWNTs on the utilization of $NaBH_4$ and the hydrogen evolution rate. It is readily observed that the $NaBH_4$ utilization increased with the increase of MWNTs content from 0 to 2 wt.% and then decreased with the further increase to 3 wt.%. Interestingly, the hydrogen formation rate exhibited an opposite trend to the utilization, which implies that the enhancement of $NaBH_4$ utilization might result from the diminished hydrogen evolution rate. The AB_5/MWNTs (2 wt.%) electrode displayed the lowest hydrogen generation rate and the highest $NaBH_4$ utilization (61.5%) among the three samples. This $NaBH_4$ utilization is higher than that reported at the Ti/Zr, Au and Pd modified AB_5-type alloy [24,26,29]. So, it can be concluded that MWNTs obviously improved that catalytic activity of AB_5 alloy and increased the utilization of $NaBH_4$ fuel.

3.2. The role of MWNTs

In order to shed light on the functioning mechanism of MWNTs in improving the catalytic performance of AB_5 alloy electrode, we analyzed the AB_5/MWNTs electrode containing 2 wt.% MWNTs using SEM and XRD. Fig. 4 shows the SEM images of the AB_5/MWNTs (2 wt.%) electrode at different magnification. It illustrated that the gaps among the AB_5-type alloy particles were filled up by MWNTs (Fig. 4a). The alloy particles were interconnected by spider web-like MWNTs (Fig. 4b) and their surfaces were also covered by the MWNTs (Fig. 4c and d). So MWNTs formed a 3D network connecting AB_5 particles together, which could enhance the electronic conductivity of the electrode. Besides, AB_5 particle surfaces can be easily accessed to the reactants via diffusion through the MWNTs network, which will lower the concentration polarization. This could be one of the reasons that the AB_5/MWNTs electrode has higher catalytic activity than AB_5 electrode.

It has been reported that the absorption of hydrogen in AB_5 alloy results in crystal cell volume increase and shifts of XRD peaks to smaller angles due to the transform from α-phase into β-phase [27,33]. In order to investigate effects of MWNTs on the hydrogen storage ability of AB_5 electrode, we immersed the AB_5 and AB_5/MWNTs (2 wt.%) electrodes in 0.1 mol dm^{-3} $NaBH_4$ and 6 mol dm^{-3} NaOH for 0.5 h and then measured their XRD spectra (Fig. 5). The un-treated AB_5 electrode was also included for comparison. As seen, the XRD patterns of AB_5 alloy before and after treatment matched well with the hexagonal $CaCu_5$ type structure (JCPDS-50-1224). For the AB_5/MWNTs (2 wt.%) electrode, the peaks at 40.5° and 43.5° obviously shifted to lower angles, which suggested that AB_5 stored more hydrogen (from the hydrolysis of $NaBH_4$, Eq. (2)) in the presence of MWNTs [27,33]. Besides, MWNTs itself can also adsorb hydrogen [34,35]. Therefore, the AB_5/MWNTs have higher hydrogen storage ability than AB_5 electrode, which explained the low hydrogen evolution rate observed at AB_5/MWNTs electrode (Fig. 3). The role of MWNTs in increasing the hydrogen storage ability was tentatively illustrated using Fig. 6. In the absence of MWNTs, less amount of hydrogen, generated by hydrolysis and incomplete electrooxidation of $NaBH_4$, can be absorbed by AB_5 (Fig. 6A). In the presence of MWNTs, it adsorbs hydrogen and some of these hydrogen can transport into AB_5 because hydrogen is thermodynamically more stable in AB_5 alloy than on MWNTs

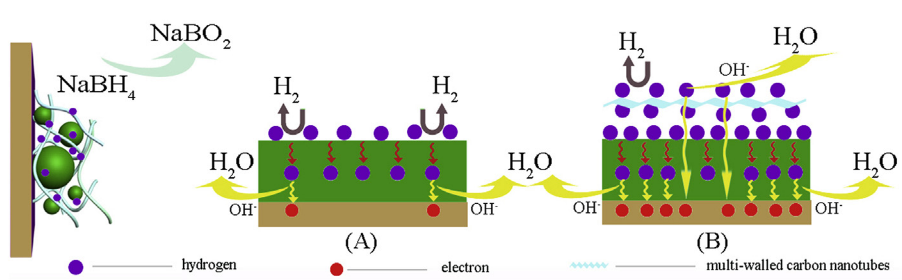

Fig. 6. A schematic depiction of the role of MWNTs during the $NaBH_4$ electrooxidation.

(Fig. 6B). The intimate contacts of MWNTs with AB_5 are important for migration of hydrogen from MWNTs to AB_5 (Fig. 4). Consequently, the AB_5/MWNTs stored more hydrogen than AB_5 alone (indicated by the XRD peak shift in Fig. 5) and thus restricted the release of hydrogen from the electrode (evidenced by the reduced hydrogen evolution rate shown in Fig. 3). The hydrogen stored in AB_5 and MWNTs can be electrooxidized during $NaBH_4$ electrooxidation. Since more hydrogen was hold in the AB_5/MWNTs than in the AB_5 electrode, the electrooxidation of these extra hydrogen leads to a higher catalytic activity and higher $NaBH_4$ utilization at the AB_5/MWNTs than at the AB_5 electrode (Figs. 1 and 3). In summary, we propose that the major role of MWNTs in the AB_5/MWNTs electrodes is that it acts as hydrogen adsorbents to diminish the release of hydrogen.

4. Conclusions

This work demonstrated that the AB_5/MWNTs (2 wt.%) electrode, simply prepared by mixing MWNTs with AB_5 alloy, exhibited a significantly higher electrocatalytic activity for $NaBH_4$ electrooxidation than the AB_5 electrode. It also shows higher $NaBH_4$ utilization and lower hydrogen evolution rate than the AB_5 electrode. This is very important for the improvement of the performance of DBFC. MWNTs attached on the AB_5 particle surfaces and formed a 3D network bridging AB_5 particles together. This increased the electronic conductivity of the electrode and made the diffusion of reactants within the electrode easier. The major role of the MWNTs is believed to be that it can adsorb hydrogen, and the adsorbed hydrogen can migrate to AB_5 alloy, thus increases the hydrogen storage capacity of the electrode and diminishes the release of hydrogen.

Acknowledgments

We gratefully acknowledge the financial support of this research by Harbin Science and Technology Innovation Fund for Excellent Academic Leaders (2012RFXXG103).

References

[1] G. Rostamikia, M.J. Janik, Energy Environ. Sci. 3 (2010) 1262–1274.
[2] D.M.F. Santos, C.A.C. Sequeira, Renew. Sustain. Energy Rev. 15 (2011) 3980–4001.
[3] B.H. Liu, Z.P. Li, J. Power Sources 187 (2009) 291–297.
[4] B.H. Liu, Z.P. Li, S. Suda, J. Power Sources 175 (2008) 226–231.
[5] J.-H. Wee, J. Power Sources 161 (2006) 1–10.
[6] G.H. Miley, N. Luo, J. Mather, R. Burton, G. Hawkins, L. Gu, E. Byrd, R. Gimlin, P.J. Shrestha, G. Benavides, J. Laystrom, D. Carroll, J. Power Sources 165 (2007) 509–516.
[7] B.H. Liu, Z.P. Li, S. Suda, J. Power Sources 185 (2008) 1257–1261.
[8] Z.P. Li, B.H. Liu, K. Arai, S. Suda, J. Electrochem. Soc. 150 (2003) A868–A872.
[9] Z.P. Li, B.H. Liu, K. Arai, S. Suda, J. Alloys Compd. 404 (2005) 648–652.
[10] D.X. Cao, Y.Y. Gao, G.L. Wang, R.R. Miao, Y. Liu, Int. J. Hydrogen Energy 35 (2010) 807–813.
[11] I. Merino-Jimenez, C.P. de Leon, A.A. Shah, F.C. Walsh, J. Power Sources 219 (2012) 339–357.
[12] K. Cheng, D.X. Cao, F. Yang, L.L. Zhang, Y. Xu, G.L. Wang, J. Mater. Chem. 22 (2012) 850–855.
[13] G. Rostamikia, A.J. Mendoza, M.A. Hickner, M.J. Janik, J. Power Sources 196 (2011) 9228–9237.
[14] E. Sanli, H. Celikkan, B.Z. Uysal, M.L. Aksu, Int. J. Hydrogen Energy 31 (2006) 1920–1924.
[15] S.C. Amendola, P. Onnerud, M.T. Kelly, P.J. Petillo, M. Binder, Selected Battery Topics. Proceedings of the Symposia, in: Electrochemical Society Proceedings, Vols. 98–15, 1999, pp. 47–54.
[16] S.I. Yamazaki, H. Senoh, K. Yasuda, Electrochem. Commun. 11 (2009) 1109–1112.
[17] M.H. Atwan, C.L.B. Macdonald, D.O. Northwood, E.L. Gyenge, J. Power Sources 158 (2006) 36–44.
[18] M.H. Atwan, D.O. Northwood, E.L. Gyenge, Int. J. Hydrogen Energy 32 (2007) 3116–3125.
[19] L.H. Yi, Y.F. Song, X. Liu, X.Y. Wang, G.S. Zou, P.Y. He, W. Yi, Int. J. Hydrogen Energy 36 (2011) 15775–15782.
[20] M.H. Atwan, D.O. Northwood, E.L. Gyenge, Int. J. Hydrogen Energy 30 (2005) 1323–1331.
[21] L.H. Yi, L. Liu, X. Liu, X.Y. Wang, W. Yi, P.Y. He, Int. J. Hydrogen Energy 37 (2012) 12650–12658.
[22] B.H. Liu, S. Suda, J. Alloys Compd. 454 (2008) 280–285.
[23] N.A. Choudhury, R.K. Raman, S. Sampath, A.K. Shukla, J. Power Sources 143 (2005) 1–8.
[24] L.B. Wang, C.N. Ma, X.B. Mao, Y.M. Sun, S. Suda, J. Mater. Sci. Technol. 21 (2005) 831–835.
[25] L.B. Wang, C.A. Ma, X.B. Mao, J. Alloys Compd. 397 (2005) 313–316.
[26] Z.Z. Yang, L.B. Wang, Y.F. Gao, X.B. Mao, C.A. Ma, J. Power Sources 184 (2008) 260–264.
[27] G.L. Wang, X.Y. Wang, R.R. Miao, D.X. Cao, K.N. Sun, Int. J. Hydrogen Energy 35 (2010) 1227–1231.
[28] G.L. Wang, W.C. Zhang, D.X. Cao, J.C. Liu, X.Y. Wang, S. Zhang, K.N. Sun, Chin. J. Chem. 27 (2009) 2166–2170.
[29] K. Cheng, Y. Xu, R.R. Miao, F. Yang, J.L. Yin, G.L. Wang, D.X. Cao, Fuel Cells 12 (2012) 869–875.
[30] S.P. Yi, H.Y. Zhang, L. Pei, Y.J. Zhu, X.L. Chen, X.M. Xue, J. Alloys Compd. 420 (2006) 312–316.
[31] S.P. Yi, H.Y. Zhang, L. Pei, S.L. Hu, L.C. Hu, Mater. Sci. Eng. B (Solid-State Mater. Adv. Technol.) 128 (2006) 125–129.
[32] X. Chen, Y. Zhang, X.P. Gao, G.L. Pan, X.Y. Jiang, J.Q. Qu, F. Wu, J. Yan, D.Y. Song, Int. J. Hydrogen Energy 29 (2004) 743–748.
[33] L. Grinberga, J. Kleperis, G. Bajars, G. Vaivars, A. Lusis, Solid State Ionics 179 (2008) 42–45.
[34] P.X. Hou, S.T. Xu, Z. Ying, Q.H. Yang, C. Liu, H.M. Cheng, Carbon 41 (2003) 2471–2476.
[35] S.C. Mu, H.L. Tang, S.H. Qian, M. Pan, R.Z. Yuan, Carbon 44 (2006) 762–767.